Observation of Stark–induced-dipole-quadrupole interference in atomic barium

S. Wielandy, T.-H. Sun,* R. C. Hilborn, and L. R. Hunter
Department of Physics, Amherst College, Amherst, Massachusetts 01002
(Received 19 June 1992)

Quantum interference between an electric-quadrupole transition and a Stark–induced-dipole-transition amplitude leads to a net orientation of an atomic excited state. When the barium $6s^2\,1S-6s5d\,{}^1D$ transition is excited in the presence of an electric field, we find the induced orientation of the $6s5d\,{}^1D$ state to be $(2.86\pm0.59)\times10^{-6}(\mathrm{V/cm})^{-1}$.

PACS number(s): 32.60.+i, 32.70.Cs, 35.80.+s

I. INTRODUCTION

A quantum interference between an electric-quadrupole transition amplitude and a Stark–induced-dipole-transition amplitude was first observed in atomic strontium [1] and then subsequently in calcium [2]. This interference effect was successfully used as a technique to determine the transition rate from the first excited ^1P state to the first excited ^1D state in each of these elements, and the results were later confirmed by other research [3–5]. In this work we report the observation of a quadrupole-Stark interference in barium and compare this result with both experiment and theory.

In this experiment, we subject barium atoms to a uniform static electric field (on the order of 2000 V/cm) along our x axis (see Fig. 1), which causes Stark mixing of the atoms' eigenstates. Of particular interest to us is the Stark mixing in the $6s^2\,{}^1S$ and the $6s5d\,{}^1D$ states. We use a "pump"-laser beam propagating along the y axis to excite the $S\rightarrow D$ transition with 877-nm light linearly polarized along the z axis. The overall transition amplitude consists of an electric-quadrupole part q which would be present even in the absence of an electric field, and an additional electric dipole part s which is brought about by the Stark mixing in the ^1S and ^1D states. A perturbation-theory calculation reveals the relative transition probabilities to the various magnetic sublevels of the ^1D state shown in Fig. 2. The sign of the quadrupole amplitude is antisymmetric with respect to the m_J quantum number of the sublevel of the ^1D state, while the sign of the Stark-induced amplitude is symmetric. The resulting interference between these amplitudes produces an orientation of the ^1D state. Hence, a measurement of the orientation of the ^1D state yields the ratio of the two amplitudes.

Since the ^1D state is metastable, the orientation created by the excitation will be lost due to collisions or precession of the polarization about stray magnetic fields before it could be observed through fluorescence. To address this problem, immediately after exciting the ^1S-^1D transition we perform a second excitation from the ^1D state to the $5d6p\,{}^1P$ state. This is accomplished with a second (probe) laser, which delivers 583-nm light also propagating along the y axis. Since this light is linearly polarized along the z axis, any orientation in the ^1D state is transferred to the ^1P state as shown in Fig. 2. When the

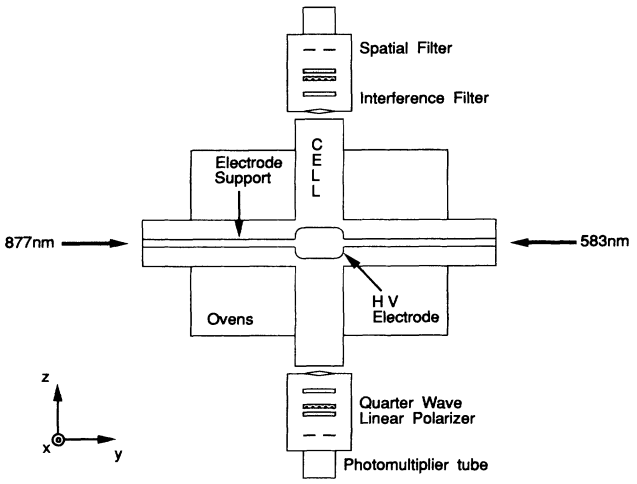

FIG. 1. Schematic diagram of the apparatus. A second identical high-voltage (HV) electrode and support is hidden below the top electrode structure shown in the figure. The laser beams and fluorescence pass between the two electrodes. The coordinate system used to describe the experiment is displayed in the lower left of the diagram.

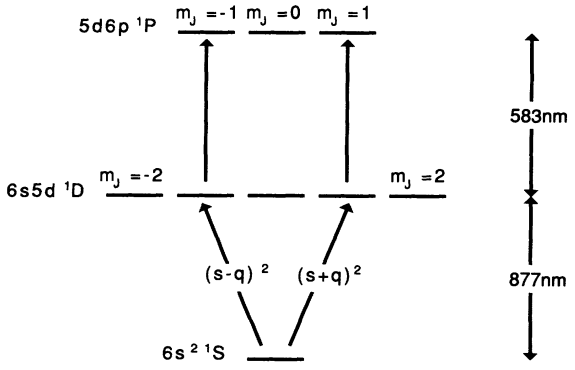

FIG. 2. Relative excitation probabilities for the magnetic sublevels. s and q represent the Stark and quadrupole amplitudes. Both lasers are linearly polarized along z.

^1P state decays to the ground state ($\lambda=350$ nm), the orientation manifests itself as a circular polarization asymmetry in the fluorescence along the z axis This asymmetry is defined to be the difference between the number of photons with $+1$ unit of angular momentum along the quantization axis and the number of photons with -1 unit of angular momentum, divided by the total number of emitted photons.

The asymmetry observed in the two senses of circularly polarized light (which is equal to twice the orientation induced in the ^1D state) is proportional (for $|s| \ll |q|$) to the ratio of the Stark to the quadrupole transition amplitudes—specifically,

$$\mathcal{A}=\frac{2s}{q} , \tag{1}$$

where $\mathcal{A}$ is the asymmetry.

The amplitudes s and q can be separated into their component angular and radial parts. The angular portions of these amplitudes can readily be evaluated, leaving the asymmetry in terms of a ratio of radial matrix elements. The asymmetry in the circularly polarized light, which we expect to observe, is described by (Ref. [1])

$$\mathcal{A}=\frac{4ceE}{\hbar\omega_{DS}^2 R_{DS}} \sum_{n\,^1P} R_{nPS}R_{DnP}\left[\frac{\omega_{nPS}}{\omega_{DnP}}+\frac{\omega_{nPD}}{\omega_{SnP}}\right] . \tag{2}$$

The summation comes from the Stark amplitude and is over all of the possible P states that are Stark mixed with the $6s5d\ ^1D$ state and the ^1S ground state. R_{ab} is the relevant radial matrix element between the two states a and b, and ω_{ab} is the angular frequency corresponding to the energy separation between these two states. E is the magnitude of the applied static electric field.

The above analysis assumes a single transition in an atom with a spin-zero nucleus. We calculate that the result [Eq. (2)] is essentially unaffected by the inclusion of the various isotopes of barium and their hyperfine structure and isotopic shifts. However, these effects do result in a small correction to our calibration signal, which will be discussed in Sec. III.

II. EXPERIMENT

We have constructed our apparatus to distinguish the Stark-quadrupole interference effect, which is linear in the applied electric field, from the Stark-induced intensity increase, which is quadratic in the electric field. We accomplish this by reversing the direction of the electric field, subtracting the asymmetry we observe with a positive electric field from that we observe with a negative one, and dividing the result by 2. Since the effect we seek to observe changes sign with the electric field, this method essentially averages two samples of the interference effect we seek while canceling the effect quadratic in the electric field.

For each orientation of the electric field, we simultaneously observe both senses of circularly polarized light emitted by placing two circular polarization detectors on opposite sides of the apparatus (Fig. 1). These detectors each consist of a photomultiplier tube, a quarter waveplate and linear polarizer combination, and both a spatial and an interference filter. The quarter waveplate is designed to rotate through 90° so that we may select the sense of circularly polarized light to which the detector will be sensitive. With the two detectors we can obtain an asymmetry measurement for each individual laser pulse. This is very important because it makes our apparatus relatively immune to observing false asymmetries caused by fluctuations in laser intensity or other external effects.

We use two dye lasers in the experiment, both pumped by a Quantel (Continuum) 660B neodymium-doped yttrium aluminum garnet (Nd:YAG) laser. The Nd:YAG laser operates at 20 Hz and delivers frequency-doubled 532-nm pulses of roughly 125 mJ and 5 ns in duration. The light used to excite the quadrupole transition is generated by a Quantel TDL 60 dye laser, fitted with dual 1800-lines/mm gratings and with LDS 867 as the lasing dye. So equipped, this laser typically produces pulses of 7.5 mJ at our wavelength.

The dye laser used to produce the 583-nm light to excite our ^1D-^1P analyzing transition is a homemade model. The laser cavity is defined by a 1200-lines/mm grating with a 500-nm blaze and a 50% reflective output mirror. An Oriel 40× telescope is used to expand the beam to the dimensions of the grating. The dye used is Rhodamine 590. With a single-stage amplifier this laser produces pulses of typically 1.5 mJ at 583 nm.

The laser light interacts with vaporized barium (heated to approximately 950 K) in an evacuated cell as shown in Fig. 1. Approximately 0.1 Torr of helium is added as a buffer gas to prevent the barium vapor from condensing on the cell windows. The spacing between the electrodes is 4.0 ± 0.1 mm, and high voltage is applied to them in microsecond pulses synchronized with the laser pulses to minimize electric discharge effects.

III. CALIBRATION

Collisions, resonance trapping, misalignments, and imperfect polarization analysis can all lead to dilutions of the observed circular polarization asymmetry. To determine the efficiency of the apparatus in detecting the atomic orientation, it is necessary to create a known orientation of the barium atoms and measure the corresponding experimental circular polarization asymmetry. The ratio of these asymmetries will then give us the analyzing power of the apparatus. To create a known orientation we apply, instead of an electric field along $\mathbf{x}$, a magnetic field of magnitude 18.9 ± 0.1 G along $\mathbf{z}$ (or $-\mathbf{z}$). If we then tune the pump laser slightly to the low-frequency side of the $^1S\rightarrow{}^1D$ resonance, we will preferentially excite those magnetic sublevels of the ^1D state that are Zeeman shifted down in energy by the magnetic field. Tuning to the high-frequency side produces the opposite effect.

We calculate the expected calibration asymmetry from the following expression:

$$\mathcal{A}=\frac{I(\nu_{\text{detuned}}-\Delta\nu)-I(\nu_{\text{detuned}}+\Delta\nu)}{I(\nu_{\text{detuned}}-\Delta\nu)+I(\nu_{\text{detuned}}+\Delta\nu)} , \tag{3}$$

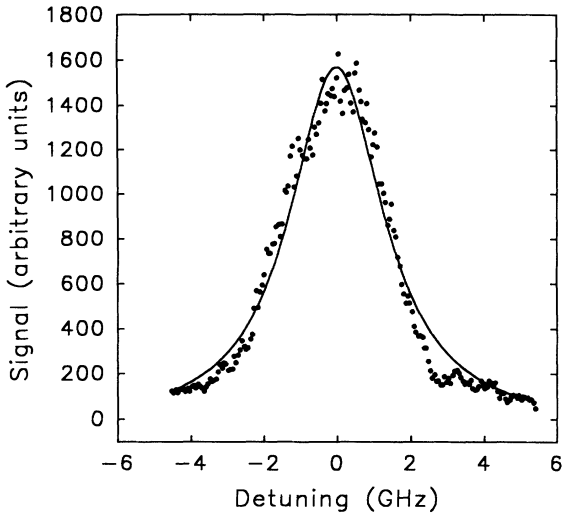

FIG. 3. Lorentzian fit of the $6s^2\,{}^1S-6s5d\,{}^1D$ transition in atomic barium.

where $I(\nu)$ is the absorption profile of the quadrupole transition and $\Delta\nu$ is the magnitude of the Zeeman shift of the relevant magnetic sublevels of the ^1D state ($m_J=\pm1$ for our choice of the pump-laser polarization along z). In order to evaluate the predicted asymmetry the absorption line shape must be known. Figure 3 shows a scan of the quadrupole transition and the best-fit Lorentzian with a full width at half maximum of 3.0 GHz. The Doppler width for this transition is 0.65 GHz at typical operating temperatures (950 K). The laser bandwidth is the dominant source of the observed absorption linewidth.

A potential complication with this calibration technique arises from the fact that the sample was not isotopically pure Ba^{138} (which is 72% abundant), but rather a naturally occurring mixture of this and the other Ba isotopes. This could affect our calibration because of the different center frequencies of the quadrupole transition in each of the isotopes and because the odd isotopes possess hyperfine structure. Though our final analysis of the calibration data takes these effects into account using the best obtainable values for hyperfine splittings [6], isotope shifts [7], and natural isotopic abundances, the deviation from the calibration expected for pure Ba^{138} was found to be only 8%.

IV. RESULTS

Data from three days of measurement is included here. The observed asymmetry and analyzing power for each days's data are shown in Table I. (The analyzing power varies from run to run due to imperfect alignment of the polarizers and primarily to changes in the barium vapor density.) Theory predicts that the asymmetry should change sign with the reversal of the propagation direction ($\mathbf{k}$) of the pump laser. Furthermore, a 90° rotation of both quarter waveplates ("polarizers +" and "polarizers −") will change the sign of the observed circular polarization asymmetry. With these signs taken into consideration, there is excellent agreement among the data

TABLE I. Data analyzed by run, detection polarizer setting, and pump-laser propagation direction.

Configuration		Normalized asymmetry/volt	Average analyzing power
Run	1	$(1.43\pm0.11)\times10^{-5}$	66%
	2	$(1.43\pm0.13)\times10^{-5}$	59%
	3	$(1.44\pm0.12)\times10^{-5}$	79%
Polarizers	+	$(1.47\pm0.10)\times10^{-5}$	64%
	−	$(1.40\pm0.10)\times10^{-5}$	78%
k	+	$(1.44\pm0.12)\times10^{-5}$	79%
	−	$(1.43\pm0.08)\times10^{-5}$	63%
Overall		$(1.43\pm0.07)\times10^{-5}$	71%

on different days and in different configurations. We have therefore compiled all of our data into a single graph depicting the asymmetry as a function of the applied voltage (Fig. 4). The total weighted average of the data in Table I yields the best-fit line shown in the figure. We assume that the intercept of the line is zero, which is clearly required since the experimental geometries for "field up" and for "field down" are identical when the electric field is zero. The slope of the line is $(1.43\pm0.07)\times10^{-5}\ \mathrm{V}^{-1}$. This result combined with the electrode spacing yields an observed asymmetry of $(5.72\pm0.31)\times10^{-6}\ (\mathrm{V/cm})^{-1}$.

In addition to the statistical uncertainties there remains the possibility of systematic uncertainties, primarily associated with the determination of the analyzing power. These uncertainties are dominated by the approximation of the absorption line profile as a Lorentzian with a 3.0-GHz linewidth. We estimate that the errors introduced by this approximation can be no larger than 20% of the observed asymmetry. If this systematic uncertainty is combined in quadrature with the statistical uncertainty, our final result for the electric-field-induced asymmetry becomes $(5.7\pm1.2)\times10^{-6}\ (\mathrm{V/cm})^{-1}$, correspond-

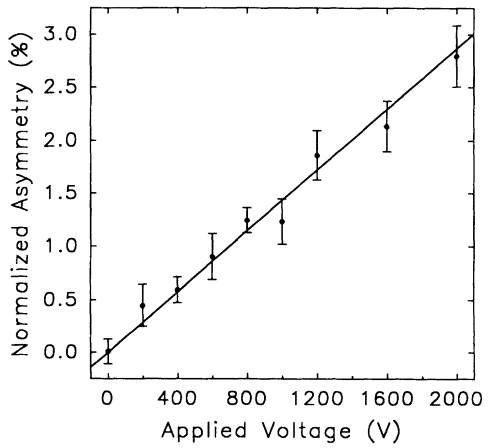

FIG. 4. Normalized asymmetry between the $m_J=+1$ and -1 sublevels of the $6s5d\,{}^1D$ state as a function of applied voltage. The electrode separation is 4.0 mm.

ing to an induced orientation of the $6s5d\ ^1D$ state of $(2.86\pm0.59)\times10^{-6}$ $(\mathrm{V/cm})^{-1}$.

V. DISCUSSION

A recent paper by Kwela and van Wijngaarden (KW) describes a related experiment [8]. In their experiment the $6s5d\ ^1D$ state of an atomic beam of Ba atoms is populated via electric discharge. The Ba atoms then move into a uniform electric-field region, where they are subjected to electric fields significantly larger than we achieve in our apparatus (on the order of 200 kV/cm). KW directly detect the fluorescence from the electric quadrupole ^1D-^1S decay and observe the difference between the signals when the electric field is on and when it is off.

Assuming that all sublevels of the ^1D state are populated equally, the KW experiment essentially measures $\frac{7}{6}(s/q)^2$ in terms of the Stark and quadrupole amplitudes. Their results imply that our asymmetry $(2s/q)$ should be $(2.14\pm0.02)\times10^{-5}$ $(\mathrm{V/cm})^{-1}$, clearly different from the value we have obtained. The origin of this discrepancy is not presently understood. We note, however, that it is possible that long-lived Rydberg levels are excited in the discharge used to populate the ^1D level in KW's work. The decay of these levels would be strongly influenced by the applied electric field and might significantly increase the observed fluorescence, either by increasing the population of the metastable D level or by creating other fluorescence that would fall within the bandpass of their detection filter.

Equation (2) shows that the measured asymmetry is determined by the relative sizes of the appropriate radial matrix elements and the (well-known) energy-level separations. The *magnitudes* of many of the matrix elements are known from measurements of the corresponding Einstein A coefficients. For the ^1S-nP and ^1D-nP matrix elements, the relationships are (Ref. [1])

$$A_{nPD}=\frac{2e^2\omega_{nPD}^3}{9\pi\hbar\epsilon_0c^3}R_{DnP}^2\ ,\quad A_{nPs}=\frac{e^2\omega_{nPS}^3}{9\pi\hbar\epsilon_0c^3}R_{sNP}^2\ . \tag{4}$$

For the ^1D-^1S electric-quadrupole transition, the appropriate relationship is

$$A_{DS}=\frac{e^2\omega_{DS}^5}{300\pi\hbar c^5\epsilon_0}R_{DS}^2\ . \tag{5}$$

While Eq. (2) involves an infinite sum, in practice we only need to know the matrix elements connecting states that are nearby in energy. However, the sum in Eq. (2) also requires the (relative) signs of the radial matrix elements. Unfortunately, knowledge of the corresponding A coefficients yields only the magnitudes of the radial matrix elements. The signs are currently unknown.

The A coefficient for the electric-quadrupole transition is reasonably well known from both theory [9,10] and experiment [11]. We use the value of 4 s^{-1} from Ref. [10] in our calculation. Table II lists the available A coefficients and wavelengths corresponding to the states that make the largest contribution to the asymmetry [12]. Unavailable A coefficients were estimated by interpolating from known values using a $1/n^3$ scaling. Also listed are the magnitudes of the contributions of each of the levels to the asymmetry.

The single largest contribution to the asymmetry comes from the $6\ ^1P$ level. A theoretical determination of the $6\ ^1P-5\ ^1D$ A coefficient is difficult due to large cancellations from different electronic configurations and large core-valence corrections [13]. These same difficulties make the determination of the sign of this matrix element

TABLE II. Transition wavelengths, A coefficients, and contributions to asymmetry for relevant Stark-mixed P states. Unless otherwise noted, A coefficients and transition wavelengths are taken from Ref. [13].

State	λ to $6s^2\ ^1S$	A_{nPS}	λ to $6s5d\ ^1D$	A_{nPD}	Contribution to asymmetry
$6s6p\ ^1P$	5.54×10^{-7}	1.15×10^{8}	1.50×10^{-6}	2.8×10^{5} [a]	1.36×10^{-5}
$6s6p\ ^3P$	7.91×10^{-7}	3.53×10^{5}	8.06×10^{-6} [b]	6.70×10^{2} [b]	3.38×10^{-6}
$5d6p\ ^1P$	3.50×10^{-7}	2.9×10^{7}	5.83×10^{-7}	9.7×10^{7}	7.05×10^{-6}
$6s7p\ ^1P$	3.07×10^{-7}	4.1×10^{7}	4.73×10^{-7}	6.9×10^{7}	3.55×10^{-6}
$6s8p\ ^1P$	2.79×10^{-7}	2.8×10^{6}	4.08×10^{-7}	4.62×10^{7} [c]	4.62×10^{-7}
$6s9p\ ^1P$	2.65×10^{-7}	1.1×10^{6}	3.79×10^{-7}	3.24×10^{7} [c]	1.89×10^{-7}
$6s10p\ ^1P$	2.54×10^{-7}	4.1×10^{6}	3.58×10^{-7}	2.37×10^{7} [c]	2.56×10^{-7}
$6s11p\ ^1P$	2.50×10^{-7}	1.5×10^{6}	3.50×10^{-7}	1.78×10^{7} [c]	1.24×10^{-7}
$6s12p\ ^1P$	2.47×10^{-7}	5.7×10^{5}	3.44×10^{-7}	1.37×10^{7} [c]	6.35×10^{-8}
$6s13p\ ^1P$	2.45×10^{-7}	6.4×10^{4}	3.41×10^{-7}	1.08×10^{7} [c]	1.81×10^{-8}
$6s14p\ ^1P$	2.44×10^{-7}	1.20×10^{5}	3.38×10^{-7}	8.63×10^{6} [c]	2.17×10^{-8}
$6s15p\ ^1P$	2.43×10^{-7}	7.80×10^{5}	3.36×10^{-7}	7.01×10^{6} [c]	4.86×10^{-8}
$6s16p\ ^1P$	2.42×10^{-7}	2.50×10^{5}	3.34×10^{-7}	5.78×10^{6} [c]	2.47×10^{-8}
$6s17p\ ^1P$	2.42×10^{-7}	1.20×10^{5}	3.33×10^{-7}	4.82×10^{6} [c]	1.54×10^{-8}
$6s18p\ ^1P$	2.41×10^{-7}	6.10×10^{4}	3.32×10^{-7}	4.06×10^{6} [c]	9.99×10^{-9}
All higher P states:					$<1.50\times10^{-7}$
				Total asymmetry not from $6s6p\ ^1P$ state:	1.53×10^{-5}

[a]Reference [14].
[b]Reference [17].
[c]Calculated using $1/n^3$ scaling.

particularly problematic. Fortunately, measurements of the (weak) branching ratio for the decay of the $6\,^1P$ level to the metastable $5D$ levels establish upper bounds on the $6\,^1P-5\,^1D$ A coefficient [14,15] that are consistent with the most recent theoretical value (Ref. [13]) of 2.8×10^5 s^{-1}.

If we assume that all terms contributing to the asymmetry have the same sign, we may calculate a maximum possible asymmetry. For the values listed in Table II, we find an asymmetry of 2.9×10^{-5} $(V/cm)^{-1}$, which is consistent with our measured value. However, more detailed conclusions are not possible without knowledge of the relative signs of the radial matrix elements.

In the interpretation of their result, KW consider only the Stark mixing of the ^1D state with the $6s6p\,^1P$ state and the $6s6p\,^3P$ state. They also neglect Stark mixing of the ^1S ground state. As shown in Table II, it is clearly inappropriate to neglect at least the next few higher ^1P states, since their contribution to the asymmetry is not at all negligible. When these terms are included, it is possible to achieve compatibility with the KW result without invoking any dramatic changes in the published theoretical A coefficients. Neglecting these terms led KW to conclude that the value of the A coefficient for the $6s6p\,^3P-6s5d\,^1D$ transition is at least an order of magnitude larger than several previous predictions would indicate [16,17].

The signs of the first several ^1P-^1S and ^1P-^1D radial matrix elements would probably enable us to resolve the conflict between the observations of KW and those of this work. Furthermore, they would allow either result to provide a more stringent check of the self-consistency of the current body of Ba A-coefficient predictions. We strongly urge that these signs be calculated.

ACKNOWLEDGMENTS

We wish to thank Phillip Grant and Daniel Krause, Jr. for important technical assistance. This work was supported by grants from the National Science Foundation, REU, RUI, and ILI programs.

*On leave from the Department of Physics, Beijing University, Beijing 100871, People's Republic of China.

[1] L. R. Hunter, W. A. Walker, and D. S. Weiss, Phys. Rev. Lett. **56**, 823 (1986).
[2] L. P. Lellouch and L. R. Hunter, Phys. Rev. A **36**, 3490 (1987).
[3] J. Kwela, Z. Phys. D **6**, 25 (1987).
[4] J. Kwela, Z. Konefal, R. Drozdowski, and J. Heldt, Z. Phys. D **9**, 215 (1988).
[5] N. Beverini, F. Giammanco, E. Maccioni, F. Strumia, and G. Vissani, J. Opt. Soc. Am. B **6**, 2188 (1989).
[6] S. G. Schmelling, Phys. Rev. A **9**, 1097 (1974).
[7] P. Grudenvik, H. Lundberg, L. Nilsson, and G. Olsson, Z. Phys. A **306**, 195 (1982).
[8] J. Kwela and A. van Wijngaarden, Phys. Rev. A **42**, 6360 (1990).
[9] J. Migdalek and W. E. Baylis, Phys. Rev. A **42**, 6897 (1990).
[10] C. W. Bauschlicher, S. R. Langhoff, R. L. Jaffe, and H. Partridge, J. Phys. B **17**, L427 (1984).
[11] I. I. Klimovskii, P. V. Minaev, and A. V. Morozov, Opt. Spektrosk. **50**, 847 (1981) [Opt. Spectrosc. (USSR) **50**, 464 (1981)].
[12] B. M. Miles and W. L. Weise, At. Data **1**, 1 (1969).
[13] C. W. Bauschlicher Jr., R. L. Jaffe, S. R. Langhoff, F. G. Mascarello, and H. Partridge, J. Phys. B **18**, 2147 (1985).
[14] D. A. Lewis, J. Kumar, M. A. Finn, and G. W. Greenlees, Phys. Rev. A **35**, 131 (1987).
[15] G. K. Gerke and B. A. Bushaw, Phys. Rev. A **37**, 1502 (1988).
[16] P. Hafner and W. H. E. Schwartz, J. Phys. B **11**, 2975 (1978).
[17] E. Trefftz, J. Phys. B **7**, L432 (1974).

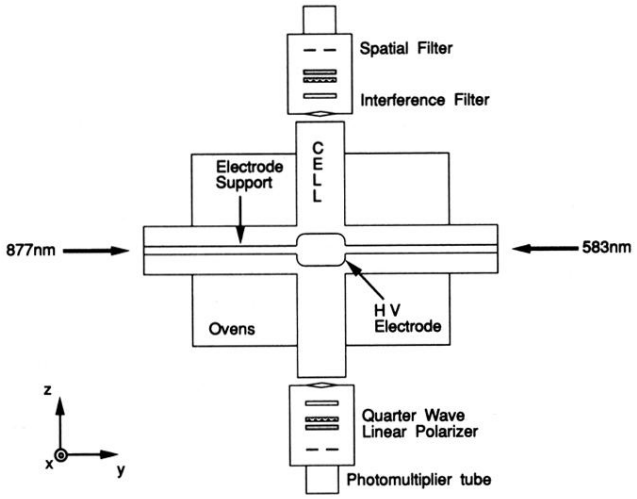

FIG. 1. Schematic diagram of the apparatus. A second identical high-voltage (HV) electrode and support is hidden below the top electrode structure shown in the figure. The laser beams and fluorescence pass between the two electrodes. The coordinate system used to describe the experiment is displayed in the lower left of the diagram.